Title:

Technical Note: Performance evaluation of volumetric imaging based on motion modeling by principal component analysis

Running title:

Volumetric imaging based on PCA

Authors:

Suzuka Asano[1], Keishi Oseki[1], Seishin Takao[2,3], Koichi Miyazaki[2,3], Kohei Yokokawa[2,3], Taeko Matsuura[2,3], Hiroshi Taguchi[4], Norio Katoh[5], Hidefumi Aoyama[5], Kikuo Umegaki[2,3], Naoki Miyamoto[2,3]

[1] Graduate School of Engineering, Hokkaido University, North 13, West 8, Kita-ku, Sapporo, Hokkaido, 060–8628, Japan.

[2] Faculty of Engineering, Hokkaido University, North13, West 8, Kita-ku, Sapporo, Hokkaido, 060–8628, Japan.

[3] Department of Medical Physics, Hokkaido University Hospital, North 14, West 5, Kita-ku, Sapporo, Hokkaido, 060–8648, Japan.

[4] Department of Radiation Oncology, Hokkaido University Hospital, North 14, West 5, Kita-ku, Sapporo, Hokkaido, 060–8648, Japan.

[5] Faculty of Medicine, Hokkaido University, North 15, West 7, Kita-ku, Sapporo, Hokkaido, 060–8638, Japan.

Corresponding author:

Naoki Miyamoto,

Faculty of Engineering, Hokkaido University, North 13, West 8, Kita-ku, Sapporo, Hokkaido, 060–8628, Japan.

Tel: +81-11-706-6673

E-mail address: miya-nao@eng.hokudai.ac.jp

Abstract

Purpose: To quantitatively evaluate the achievable performance of volumetric imaging based on lung motion modeling by principal component analysis (PCA).

Methods: In volumetric imaging based on PCA, internal deformation was represented as a linear combination of the eigenvectors derived by PCA of the deformation vector fields evaluated from patient-specific four-dimensional-computed tomography (4DCT) datasets. The volumetric image was synthesized by warping the reference CT image with a deformation vector field which was evaluated using optimal principal component coefficients (PCs). Larger PCs were hypothesized to reproduce deformations larger than those included in the original 4DCT dataset. To evaluate the reproducibility of PCA-reconstructed volumetric images synthesized to be close to the ground truth as possible, mean absolute error (MAE), structure similarity index measure (SSIM) and discrepancy of diaphragm position were evaluated using 22 4DCT datasets of nine patients.

Results: Mean MAE and SSIM values for the PCA-reconstructed volumetric images were approximately 80 HU and 0.88, respectively, regardless of the respiratory phase. In most test cases including the data of which motion range was exceeding that of the modeling data, the positional error of diaphragm was less than 5 mm. The results suggested that large deformations not included in the modeling 4DCT dataset could be reproduced. Furthermore, since the first PC correlated with the displacement of the diaphragm position, the first eigenvector became the dominant factor representing the respiration-associated deformations. However, other PCs did not necessarily change with the same trend as the first PC, and no correlation was observed between the coefficients. Hence, randomly allocating or sampling these PCs in expanded ranges may be applicable to reasonably generate an augmented dataset with various deformations.

Conclusions: Reasonable accuracy of image synthesis comparable to those in the previous research were shown by using clinical data. These results indicate the potential of PCA-based volumetric imaging for clinical applications.

KEYWORDS

Volumetric imaging, principal component analysis, motion modeling, data augmentation, respiratory motion

1 INTRODUCTION

Volumetric imaging[1-13], which can visualize three-dimensional (3D) anatomical structures during treatment, is expected to be clinically practical as a motion management technique in radiation therapy. Some studies regarding volumetric imaging are based on motion modeling with principal component analysis (PCA). In PCA-based motion modeling[2-4,7,9,12,14], internal deformation is represented as a linear combination of the eigenvectors derived by the PCA of the deformation vector field evaluated from patient-specific four-dimensional-computed tomography (4DCT) datasets. The volumetric image can be synthesized by warping the reference computed tomography (CT) image with a deformation vector field evaluated with optimal principal component coefficients (PCs), serving as eigenvector weights. Some techniques to estimate optimum PCs during treatment have been reported. One is based on minimizing the difference between the digitally reconstructed radiographs created from the synthesized CT and actual fluoroscopic images[4]. Another one is based on the correlation model between PCs and external surrogate information[2]. Recently, a method using convolutional neural networks (CNNs) has also been proposed[7]. In this approach, PCA was also applied for data augmentation to generate the training dataset, including various deformations.

PCA has been applied for volumetric imaging and data augmentation in deep learning, as described in the last paragraph. Although, it is crucial to quantitatively evaluate the achievable performances of volumetric imaging based on PCA to support clinical feasibility, only a few reports on validation with clinical datasets simulating actual clinical situations such as the motion difference between treatment and 4DCT acquisition. Therefore, this study quantitatively evaluated the performance of PCA-based volumetric imaging using multiple clinical 4DCT datasets.

2 MATERIALS AND METHODS

2.1 PCA-based motion modeling

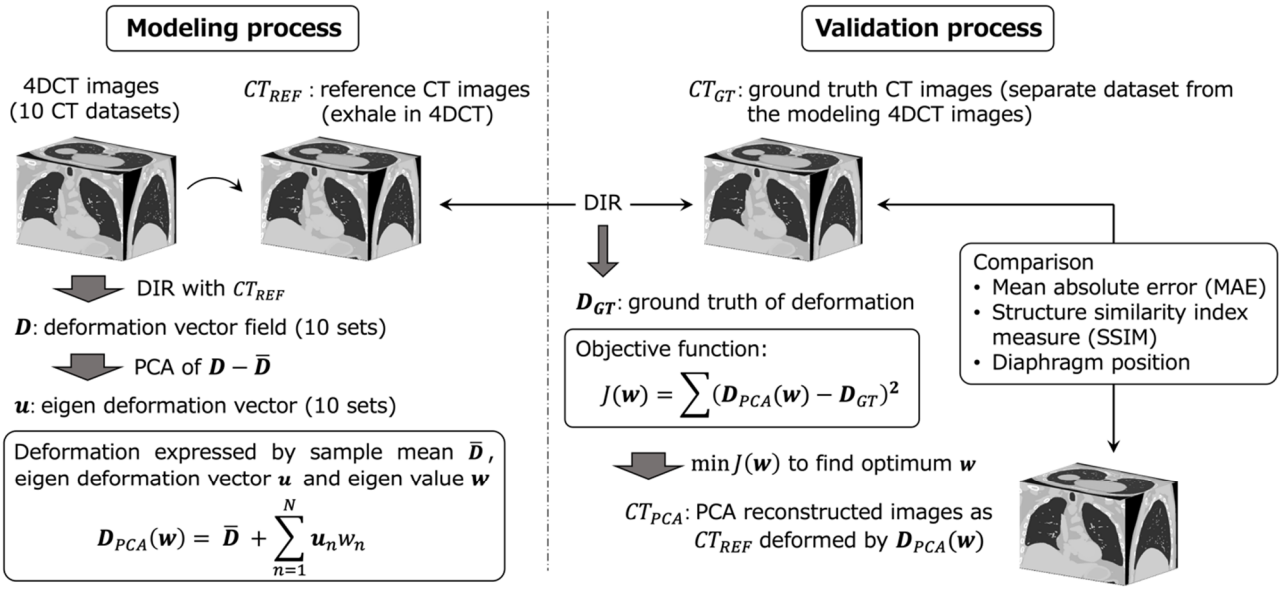

FIGURE 1 Schematic showing the PCA-based motion modeling and validation processes in this study.

The PCA-based motion modeling process is shown in Fig. 1. First, the deformation vector field ($\boldsymbol{D}$) was evaluated using the deformable image registration (DIR) with each CT data. The CT data at the expiratory phase of the 4DCT dataset (10 CT datasets for one respiratory cycle) were the reference (CT_{Ref}). Furthermore, the number of rows and columns of $\boldsymbol{D}$ was the number of voxels multiplied 3 (# of deformation directions) and 10 (# of respiratory phase bins), respectively. Subsequently, the column vector ($\bar{\boldsymbol{D}}$) was evaluated as the sample mean of $\boldsymbol{D}$. Then, eigenvectors $\boldsymbol{u}_1, \boldsymbol{u}_2, \dots, \boldsymbol{u}_{10}$ were obtained using the PCA of $\boldsymbol{D} - \bar{\boldsymbol{D}}$. Finally, using N principal eigenvectors, the internal deformation was expressed as follows.

$$\boldsymbol{D}_{PCA}(\boldsymbol{w}) = \bar{\boldsymbol{D}} + \sum_{n=1}^{N} \boldsymbol{u}_n w_n$$

where $\boldsymbol{w} = (w_1, w_2, \dots, w_n)$ is the principal component coefficient (PC). By warping CT_{Ref} with $\boldsymbol{D}_{PCA}(\boldsymbol{w})$, a volumetric image can be generated as a CT image. Larger PCs can then reproduce internal deformations larger than those not included in the original 4DCT dataset.

2.2 Patient data

Twenty-two 4DCT datasets of nine patients with relatively small motion artifacts from The Cancer Image Archive[15,16] were used. This study assumed that these 4DCT datasets had been acquired during normal breathing at rest because the motion artifacts were small. Two or three 4DCT datasets were included for each patient. The displacement of the right diaphragm position for each 4DCT dataset is shown in Fig. 2, indicating the respiratory motion range. To evaluate the performance of PCA-based motion modeling in case of the larger deformations not included in the modeling data, the 4DCT dataset with smaller diaphragm displacements and the other 4DCT datasets were used as modeling data to derive eigenvectors and validation data, respectively. Hence, PCA-based motion model is created for each patient. The resolution of the CT data was 0.98 mm/pixel. The slice thickness was resampled from the original 3 mm to 1 mm. In the DIR function used in this study, one smoothing factor is applied to all three axes. Hence, slice thickness was resampled to 1 mm which was same as pixel size in order to equalize the smoothing effect to all axes. To avoid the influence of anatomical changes that eigenvectors could not reproduce, such as weight changes during the treatment course, the 4DCT datasets for modeling and validation were selected within 1 month. Additionally, because the patient setup position in each 4DCT acquisition was different, six-axis rigid image registration was performed in the spinal cord region, which was considered rigid, using the 4DCT dataset on the oldest date as a reference. Based on visual inspection of the registered images, it was confirmed that the anatomical variation between the 4DCT images acquired on different days was mainly induced by the respiration.

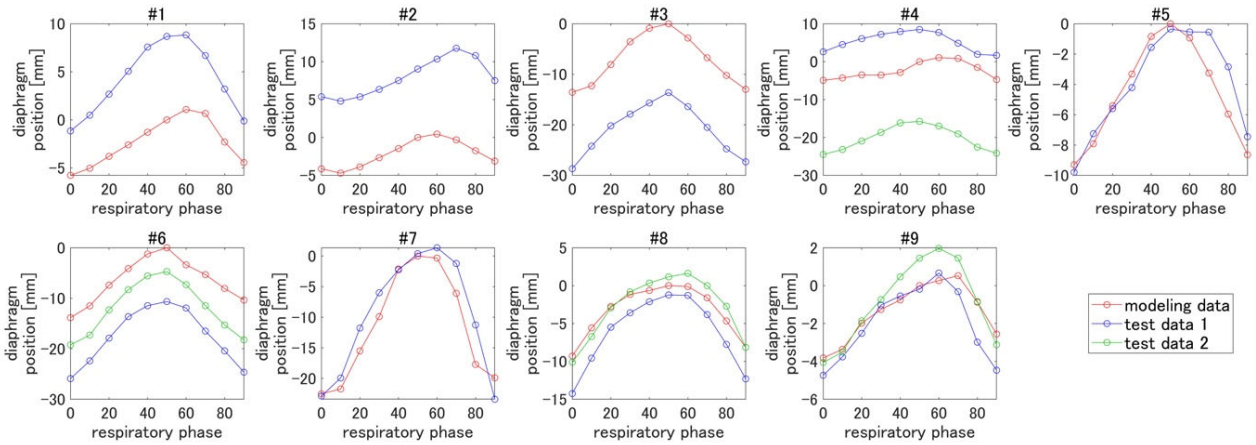

FIGURE 2 Displacement of the diaphragm position for each respiratory phase in nine patients. The displacement was evaluated on the basis of the phase 50 (expiration) in the modeling data.

2.3 Evaluation of PCA-based lung deformation modeling

The validation process is shown on the right side of Fig. 1. In this study, MATLAB (MathWorks Inc, USA) was used for processing the DICOM (Digital Imaging and Communications in Medicine) format image, DIR, and quasi-Newton method to find the optimal PCs. The deformation vector field obtained by DIR between the CT image (defined as the ground truth: CT_{GT}) obtained on a different date from the modeling 4DCT dataset and the reference CT image (CT_{Ref}) included in the modeling 4DCT dataset was defined as the ground truth of deformation ($\boldsymbol{D}_{GT}$). In this study, the number of PCs was set to three as in previous studies (i.e. $\boldsymbol{w} = [w_1, w_2, w_3]$), to consider the modeling accuracy and overfitting balance. It has been confirmed that using three or more principal components resulted in an accumulated contribution rate more than 80% for each patient. Then, the objective function was defined as the sum of the absolute differences between $\boldsymbol{D}_{GT}$ and $\boldsymbol{D}_{PCA}(\boldsymbol{w})$:

$$J(\boldsymbol{w}) = \sum (\boldsymbol{D}_{PCA}(\boldsymbol{w}) - \boldsymbol{D}_{GT})^2$$

After the PCs ($\boldsymbol{w}$) that minimize $J(\boldsymbol{w})$ were obtained using the quasi-Newton method, the CT image (CT_{PCA}) was synthesized by warping the reference image (CT_{REF}) by the deformation $\boldsymbol{D}_{PCA}(\boldsymbol{w})$, followed by evaluation with the optimum coefficient. In this way, CT_{PCA} could be synthesized using the deformation closest to the ground truth.

This study evaluated the performance of PCA-based volumetric imaging by comparing CT_{PCA} with CT_{GT}. The reproducibility of CT values and anatomical structures were evaluated using mean absolute error (MAE) and structure similarity index measure (SSIM), respectively. MAE was evaluated as:

$$\text{MAE} = \frac{1}{n}\sum_{i=1}^{n} |I_i - I_i^*| \ ,$$

where I_i^* is the actual CT value at voxel i in the ground truth image, I_i is the CT value at voxel i in the

synthesized image, and n is voxel number. SSIM which is commonly used in pattern matching as a measure of the similarity of image structures was evaluated as:

$$\mathrm{SSIM} = \frac{(2\mu_x\mu_y + C_1)(2\sigma_{xy} + C_2)}{(\mu_x^2 + \mu_y^2 + C_1)(\sigma_x^2 + \sigma_y^2 + C_2)},$$

where μ_x and μ_y are the average CT values in ground truth image and synthesized image respectively, σ_x and σ_y are variance of CT value in ground truth image and synthesized image respectively, and σ_{xy} is a covariance of ground truth image and synthesized image. C_1 and C_2 were defined as $C_1 = (0.01 \times L)^2$ and $C_2 = (0.03 \times L)^2$, respectively. L was dynamic range of the image and was defined as the maximum CT value in the ground truth image.

In addition, discrepancy of the diaphragm position between ground truth image and PCA-reconstructed image was evaluated as positional accuracy. The diaphragm position was evaluated with the same area with motion range evaluation shown in Fig.2.

3 RESULTS

3.1 MAE of PCA-reconstructed volumetric image

An example of PCA-reconstructed volumetric images with assuming CT data at respiratory phase 0 in test data 2 of patient 6 as the ground truth are shown in Fig. 3. We observed that the difference in diaphragm positions between the reference and ground truth images was approximately 20 mm (see the second column from the right in Fig. 3). As shown in Fig. 2, the diaphragm position at respiratory phase 0 in test data 2 of patient 6 exceeded 5 mm from that in the modeling data. MAE and SSIM, in this case, were 89.0 HU and 0.85, respectively, approximately an average of all evaluated cases. Although there was a discrepancy around the diaphragm dome, the overall synthesized image was close to the actual, including that of the tumor, position and shape.

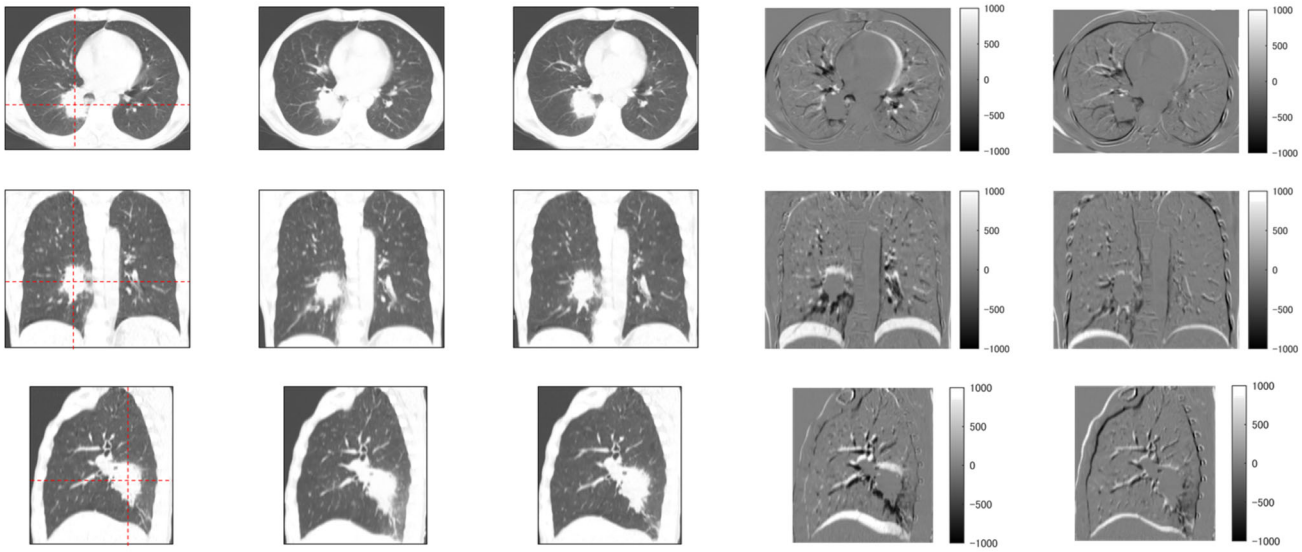

FIGURE 3 From the left row: reference image (image to be deformed), ground truth image (respiratory phase 0 in test data 2 of patient 6), PCA-reconstructed volumetric image, difference between reference and ground truth images, and difference between PCA-reconstructed volumetric and ground truth images. From top to bottom: axial, coronal, and sagittal images. The dashed line in the reference image indicates the slice position at the tumor center.

The MAE between PCA-reconstructed volumetric image and ground truth images for each respiratory phase is shown in Fig. 4. Subsequently, the MAE between the reference and ground truth images was also evaluated to show the difference between the original nondeformed reference and the ground truth. Since the expiratory phase was used as the reference image, we observed that the MAE of the reference image was larger in the inspiratory phase, whereas the deformation was relatively large. The mean MAE of the PCA-reconstructed volumetric images for each respiratory phase was approximately 80 HU, and its accuracy was maintained even in the inspiratory phase. These results suggest that PCA could reproduce large deformations not included in the modeling data during normal breathing at rest. Moreover, the MAE appeared large in the validation data containing deformations that were difficult to model with PCA, for example the deformations were different in the left and right lungs.

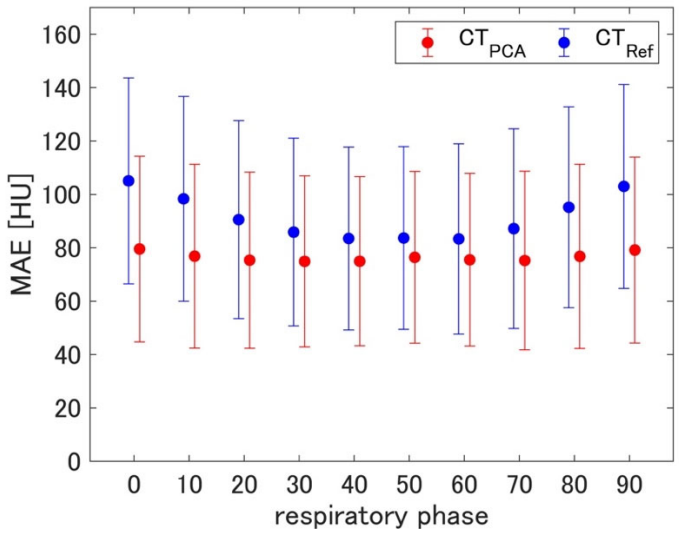

175

176 **FIGURE 4** MAE of PCA-reconstructed volumetric image and reference image for the 13 cases from nine

177 patients at each respiratory phase.

178

179 **3.2 SSIM of PCA-reconstructed volumetric image**

180 The SSIM at each respiratory phase is shown in Fig. 5. As in the evaluation of the MAE, the SSIM between

181 the reference and ground truth images was also evaluated. Since the expiratory phase was used as a reference,

182 the SSIM of the reference image was decreased on the inspiratory phase. Alternatively, the mean SSIM of the

183 PCA-reconstructed volumetric images was approximately 0.88 for each respiratory phase, maintaining a high

184 structural reproducibility, even in the inspiratory phase.

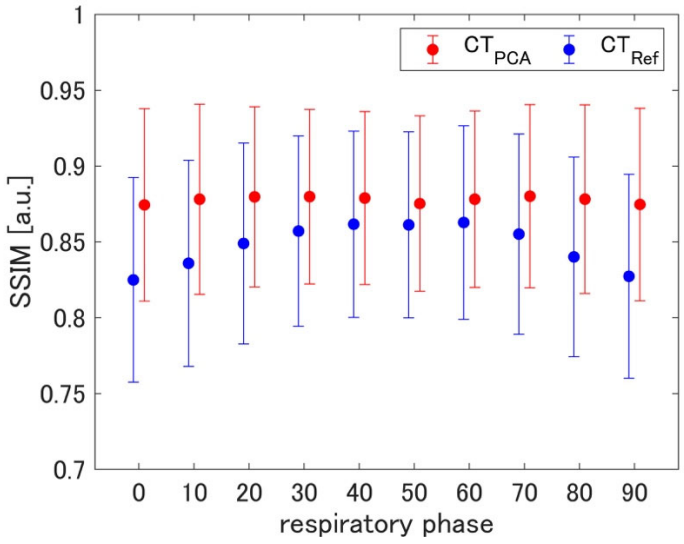

185

FIGURE 5 SSIM of PCA-reconstructed volumetric image and reference image for the 13 cases from nine patients at each respiratory phase.

3.3 Positional accuracy of PCA-reconstructed volumetric image

Discrepancy of the diaphragm position between ground truth image and PCA-reconstructed image is shown in Fig.6. In most cases, the positional error of diaphragm was less than 5 mm. As shown in #1, #2, #3, #4, and #6 in Fig.2, the motion range of half the test data exceeded that of the modeling data. Therefore, these results suggested the possibility that PCA-based volumetric imaging could be applied to synthesize images even when the motion is exceeded from the modeling data. In addition, since the diaphragm is the region that moves the most due to breathing, the positional error in the lung region is expected to be smaller than that in the diaphragm.

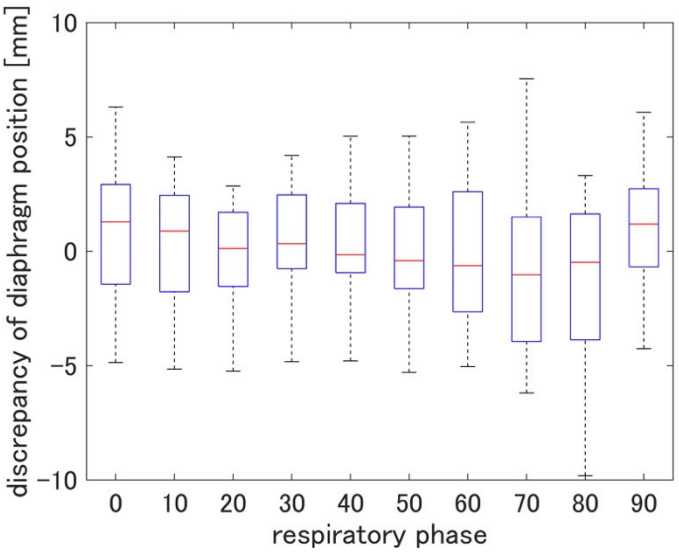

FIGURE 6 Discrepancy of the diaphragm position between ground truth image and PCA-reconstructed image for the 13 cases from nine patients at each respiratory phase.

4 DISCUSSION

This study quantitatively evaluated the achievable reproducibility of PCA-based volumetric imaging. The mean values of MAE and SSIM of the PCA-reconstructed volumetric images were approximately 80 HU and 0.88, respectively, regardless of the respiratory phase, and were comparable with those evaluated in previous

studies[5,8], using the same 4DCT dataset or digital phantoms. These results suggest that volume images could be synthesized with reasonable accuracy if the optimal PCs could be estimated even when the treatment motion differs from that observed during 4DCT acquisition.

In deep learning-based techniques, which is based on a CNN to estimate PCs from the X-ray fluoroscopic images, training data is generated by data augmentation with applying various PCs. The quality of the training data is one of the most important factors that determine the performance of the volumetric imaging. That is, in the data augmentation, the data which could be clinically observed should be included for the effective training of CNN. In order to understand actual distribution of PCs in clinical cases, the three PCs that reproduced deformation closest to the ground truth were evaluated as shown in Fig. 7. Because the first PC (PC1) correlated with the displacement of the diaphragm position (Fig. 2), the first eigenvector was proposed as the dominant factor representing the deformation associated with respiration. However, the second and third PCs did not necessarily change with the same trend as PC1, and no correlation was observed between the coefficients. This result suggests that equally scaling all coefficients alone does not necessarily reproduce clinical data with large deformation beyond the original modeling data. Considering that no clear correlation existed between PCs, randomly allocating PCs[7] or sampling PCs in expanded ranges to generate various deformations could be a solution for data augmentation.

This study evaluated optimal PCs as the coefficients that minimize the difference between the internal deformations represented as the linear combination of eigenvectors and the ground truth of deformation. Although PC estimation methods are different in clinical practice, PC1 with the largest contribution is expected to be similarly estimated because it strongly correlates with respiratory motion. Therefore, the synthesized volume images could be applied to confirm the target location and evaluate the consistency of the internal structures between the planned and synthesized CT images as a motion management technique.

There were some error sources in this PCA-based volumetric imaging. One error source was the variation in the patient's breathing patterns. Assuming that the 4DCT data were acquired during normal breathing at rest, it could be challenging to reproduce deformation patterns different from those obtained during 4DCT acquisition, such as during forced breathing using additional muscles. Motion artifacts in 4DCT may also be an error source,

231 although the reconstruction algorithm could compensate for it[17,18]. The anatomical variation during the treatment
232 course, which cannot be evaluated from the 4DCT dataset, is also an error source. Therefore, it may be useful
233 to evaluate body shape changes with a 3D body surface measurement system and retake a 4DCT/four-
234 dimensional cone beam CT image to update the model. Tumor shrinkage or growth is also challenging to
235 reproduce with the PCA of the 4DCT dataset. Nevertheless, a method to simulate the tumor shape variation
236 based on image warping could be applicable[5].

237

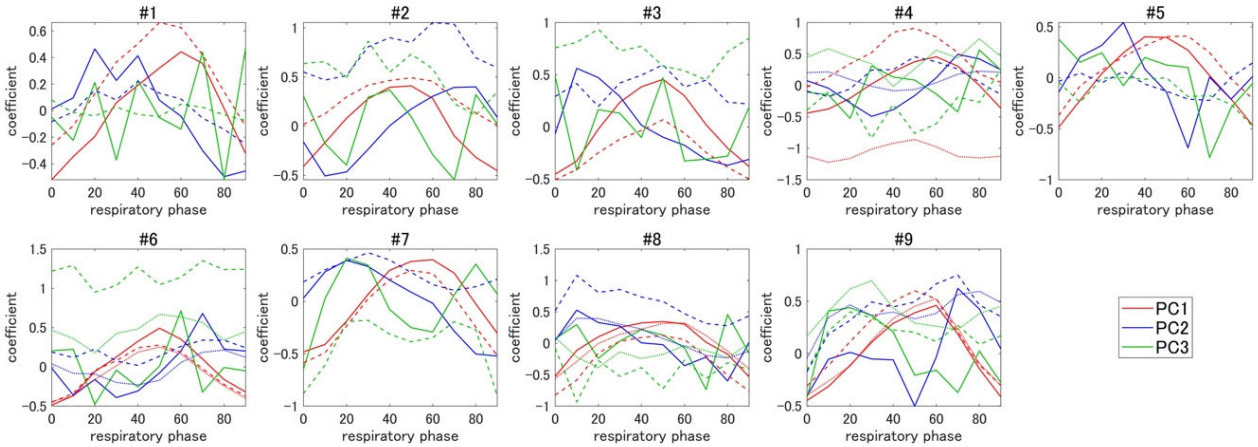

238

239 **FIGURE 7** Three principal component coefficients (PCs) that reproduced the deformation closest to the
240 ground truth. Solid, dashed, and dotted lines represent evaluations of the modeling test data 1 and 2.

241

242 # 5 CONCLUSIONS

243 This study quantitatively evaluated the achievable performance of volumetric imaging based on PCA using
244 multiple patient 4DCT datasets acquired on different dates. The mean MAE and SSIM of the PCA-reconstructed
245 volumetric images were approximately 80 HU and 0.88, respectively, regardless of the respiratory phase. In
246 most test cases including the data of which motion range was exceeding that of the modeling data, the positional
247 error of diaphragm was less than 5 mm. These results suggest that volume images could be synthesized with
248 reasonable accuracy for clinical applications by estimating the optimal PCs.

249

250 **ACKNOWLEDGMENT**

This research was partially supported by AMED under Grant Number JP20he2302001 and KAKENHI 20H03612.

REFERENCE

1. Fassi A, Seregni M, Riboldi M, et al. Surrogate-driven deformable motion model for organ motion tracking in particle radiation therapy [published online ahead of print 2015/01/24]. *Phys Med Biol.* 2015;60(4):1565-1582.
2. Lafreniere M, Mahadeo N, Lewis J, Rottmann J, Williams CL. Continuous generation of volumetric images during stereotactic body radiation therapy using periodic kV imaging and an external respiratory surrogate [published online ahead of print 2019/06/22]. *Phys Med.* 2019;63:25-34.
3. Mishra P, Li R, James SS, et al. Evaluation of 3D fluoroscopic image generation from a single planar treatment image on patient data with a modified XCAT phantom [published online ahead of print 2013/01/23]. *Phys Med Biol.* 2013;58(4):841-858.
4. Li R, Jia X, Lewis JH, et al. Real-time volumetric image reconstruction and 3D tumor localization based on a single x-ray projection image for lung cancer radiotherapy [published online ahead of print 2010/07/17]. *Med Phys.* 2010;37(6):2822-2826.
5. Lei Y, Tian Z, Wang T, et al. Deep learning-based real-time volumetric imaging for lung stereotactic body radiation therapy: a proof of concept study [published online ahead of print 2020/10/21]. *Phys Med Biol.* 2020;65(23):235003.
6. Giger A, Krieger M, Jud C, et al. Liver-ultrasound based motion modelling to estimate 4D dose distributions for lung tumours in scanned proton therapy [published online ahead of print 2020/07/30]. *Phys Med Biol.* 2020;65(23):235050.
7. Wei R, Zhou F, Liu B, et al. Convolutional Neural Network (CNN) Based Three Dimensional Tumor Localization Using Single X-Ray Projection. *IEEE Access.* 2019;7:37026-37038.
8. Hayashi R, Miyazaki K, Takao S, et al. Real-time CT image generation based on voxel-by-voxel modeling of internal deformation by utilizing the displacement of fiducial markers [published online ahead of print 2021/07/15]. *Med Phys.* 2021;48(9):5311-5326.
9. Zhang Q, Pevsner A, Hertanto A, et al. A patient-specific respiratory model of anatomical motion for radiation treatment planning [published online ahead of print 2008/01/17]. *Med Phys.* 2007;34(12):4772-4781.
10. Li R, Lewis JH, Jia X, et al. On a PCA-based lung motion model [published online ahead of print 2011/08/26]. *Phys Med Biol.* 2011;56(18):6009-6030.
11. Zhang Y, Knopf AC, Weber DC, Lomax AJ. Improving 4D plan quality for PBS-based liver tumour treatments by combining online image guided beam gating with rescanning [published online ahead of print 2015/10/07]. *Phys Med Biol.* 2015;60(20):8141-8159.
12. Zhang Y, Knopf A, Tanner C, Lomax AJ. Online image guided tumour tracking with scanned proton

beams: a comprehensive simulation study [published online ahead of print 2014/11/25]. *Phys Med Biol.* 2014;59(24):7793-7817.

13. Xu Y, Yan H, Ouyang L, et al. A method for volumetric imaging in radiotherapy using single x-ray projection [published online ahead of print 2015/05/17]. *Med Phys.* 2015;42(5):2498-2509.
14. Yan H, Wang X, Yin W, et al. Extracting respiratory signals from thoracic cone beam CT projections [published online ahead of print 2013/02/13]. *Phys Med Biol.* 2013;58(5):1447-1464.
15. Hugo GD, Weiss E, Sleeman WC, et al. Data from 4D Lung Imaging of NSCLC Patients. The Cancer Imaging Archive. 2016;http://doi.org/10.7937/K9/TCIA.2016.ELN8YGLE.
16. Hugo GD, Weiss E, Sleeman WC, et al. A longitudinal four-dimensional computed tomography and cone beam computed tomography dataset for image-guided radiation therapy research in lung cancer [published online ahead of print 2016/12/20]. *Med Phys.* 2017;44(2):762-771.
17. Gianoli C, Riboldi M, Spadea MF, et al. A multiple points method for 4D CT image sorting [published online ahead of print 2011/04/02]. *Med Phys.* 2011;38(2):656-667.
18. Spadea MF, Baroni G, Gierga DP, Turcotte JC, Chen GT, Sharp GC. Evaluation and commissioning of a surface based system for respiratory sensing in 4D CT [published online ahead of print 2011/02/19]. *Journal of applied clinical medical physics / American College of Medical Physics.* 2010;12(1):3288.